Highly conducting poly(methyl methacrylate) / carbon nanotubes composites: Investigation on their thermal, dynamic-mechanical, electrical and dielectric properties

E. Logakis, Ch. Pandis, P. Pissis, J. Pionteck, P. Pötschke

Highly conducting poly(methyl methacrylate) / carbon nanotubes composites: Investigation on their thermal, dynamic-mechanical, electrical and dielectric properties

E. Logakis, Ch. Pandis, P. Pissis, J. Pionteck, P. Pötschke

PII: S0266-3538(11)00057-1
DOI: 10.1016/j.compscitech.2011.01.029
Reference: CSTE 4924

To appear in: *Composites Science and Technology*

Received Date: 4 August 2010
Revised Date: 24 January 2011
Accepted Date: 30 January 2011

Please cite this article as: Logakis, E., Pandis, Ch., Pissis, P., Pionteck, J., Pötschke, P., Highly conducting poly(methyl methacrylate) / carbon nanotubes composites: Investigation on their thermal, dynamic-mechanical, electrical and dielectric properties, *Composites Science and Technology* (2011), doi: 10.1016/j.compscitech.2011.01.029

Highly conducting poly(methyl methacrylate) / carbon nanotubes composites: Investigation on their thermal, dynamic-mechanical, electrical and dielectric properties

E. Logakis[1*], Ch. Pandis[1], P. Pissis[1], J. Pionteck[2], P. Pötschke[2]

[1]*National Technical University of Athens, Zografou Campus, 15780, Athens, Greece*

[2]*Leibniz Institute of Polymer Research Dresden, 01069 Dresden, Germany*

[*]Current Affiliation: Cranfield University, Composites Centre, Cranfield, Bedfordshire MK43 0AL, UK

E-mail: e.logakis@cranfield.ac.uk, Tel.: +44 (0) 1234 750111 ext 2408, Fax: +44 (0) 1234 752473

Abstract

Nanocomposites of poly(methyl methacrylate) (PMMA) containing various multi-walled carbon nanotubes (MWCNT) contents were prepared using melt mixing. Several techniques were employed to study the influence of the MWCNT addition on the thermal, mechanical, electrical and dielectric properties of the PMMA matrix. The electrical percolation threshold (p_c) was found to be 0.5 vol.% by performing AC and DC conductivity measurements. Significantly high conductivity levels (σ_{dc}) were achieved: σ_{dc} exceeds 10^{-2} S/cm already at 1.1 vol.%, the criterion for EMI shielding ($\sigma_{dc} > 10^{-1}$ S/cm) is fulfilled at 2.9 vol.%, and the highest loaded sample (5.2 vol.%) gave a maximum value of 0.5 S/cm. Dielectric relaxation spectroscopy measurements in broad frequency (10^{-1}–10^{6} Hz) and temperature ranges (-150 to 170 ºC) indicated weak polymer-filler interactions, in consistency with differential scanning calorimetry and dynamic mechanical analysis findings. Weak polymer-filler interactions and absence of crystallinity facilitate the achievement of high conductivity levels in the nanocomposites.

Keywords:
A. Nano composites
A. Carbon Nanotubes
B. Electrical properties
B. Thermomechanical properties

1. Introduction

Carbon nanotube-based polymer composites have drawn tremendous interest in both research and industry communities as the dramatic increase of published articles in this field, especially during the last decade, clearly shows [1,2]. The unique thermal, mechanical and electrical properties of carbon nanotubes (CNT) in combination with their small size scale, low mass density and high aspect ratio, makes them ideal reinforcing agents for numerous applications [3]. From 1994, when Ajayan et al. first incorporate CNT in an epoxy matrix [4], till now, CNT have been used as fillers in all the available polymer matrices, aiming mainly to improve their mechanical and electrical properties, as well as their thermal stability [5,6]. Amongst them, poly(methyl methacrylate) (PMMA) is of special interest due to its amorphous nature, optical clarity and biocompatibility. PMMA/CNT composites can found application as electromagnetic interference (EMI) shielding materials [7-9], transparent conducting films [10-12], gas sensors [13,14], etc. In addition, functionalization of CNT can significantly enhance the thermal and mechanical properties of PMMA [15-18]. It should be noted that the attachment of functional groups onto the CNT walls, from one hand enhances the interfacial adhesion between the matrix and the fillers [18], facilitating the dispersion of CNT [16,17], whereas, on the other hand, disrupts the π-bonds of the graphite lattice, which contribute the delocalized electrons, resulting in decreased values of conductivity in the composites [19].

Literature survey in conducting PMMA/CNT systems reveals several works prepared by the common methods of solution mixing/casting [7-9,11,12,20-24] and in-situ polymerization [8,9,25], and a limited number of studies where other more sophisticated techniques were employed (coagulation [26,27], electrospinning [28], latex technology

[29], combination of solvent casting and melt mixing [30]). Surprisingly, there are only few works in systems prepared by melt mixing, even though this method has been widely applied in other thermoplastic matrices, since it offers several advantages such as speed, simplicity, low cost, absence of solvents and availability of the required equipment in the plastic industry. In particular, Jin et al. reported a delay in the onset of thermal degradation and a significant increase of storage modulus of PMMA, especially in the rubbery state, in PMMA/CNT composites fabricated by melt mixing [31]. Gorga et al. described a large improvement in the tensile toughness, in the range of 170%, in oriented to the draw direction PMMA/CNT composites [32]. Furthermore, McClory et al. studied the electrical and rheological properties of PMMA/CNT composites, having as parameters the size of the PMMA grains used during mixing, and the aspect ratio and functionality of CNT [19]. To the best of our knowledge, the latter work is the only one referring to the electrical properties of melt mixed PMMA/CNT composites.

In this study PMMA/CNT composites were prepared using melt mixing. As fillers non functionalized multi-walled carbon nanotubes (MWCNT) were used, aiming in the preparation of highly conducting composites. The electrical properties are studied and the electrical percolation threshold (p_c), being the critical composition of conducting inclusions where the first network is formed, is derived at room temperature using dielectric relaxation spectroscopy (DRS) and four-point probe *dc* conductivity measurements. The achieved conductivity levels are discussed and compared with previously mentioned ones in several amorphous and semicrystalline systems containing the same type of MWCNT like here; the role of conductivity is highlighted. Furthermore, the morphological, thermal and mechanical properties are investigated by employing scanning electron microscopy (SEM),

differential scanning calorimetry (DSC) and dynamic mechanical analysis (DMA), respectively, in an essay for understanding their structure – property relationships scheme. Finally, the influence of MWCNT on the molecular dynamics of PMMA matrix is examined by DRS, in a wide frequency and temperature range, giving valuable information about the polymer-filler interactions in the nanocomposites.

2. Experimental

2. 1. Materials

PMMA Plexiglas® 7N (density: 1.19 g/cm^3) from Röhm GmbH & Co. KG (Germany), was used in pellet form. Multi-walled carbon nanotubes (MWCNT) Nanocyl^{TM} NC7000 (density: 1.66 g/cm^3 [33]) were supplied from Nanocyl S.A. (Sambreville, Belgium). The nanotubes were produced by the chemical vapour deposition (CVD) method (average diameter 9.5 nm, average length 1.5 μm, carbon purity >95 %) [34].

The nanocomposites were prepared by melt mixing. Prior to mixing, all the materials were dried in an oven under vacuum (PMMA: 80 °C for 2-3 h, MWCNT: 120 °C for 2 h). The mixing was done in a DACA-Micro Compounder at 230°C, for 10 min, at a mixing speed of 100 rpm. The extruded strands were pressed into sheets using a Vogt LaboPress 200T at 230 °C, 10 bar, for 1 min (preheating of the material at 230 °C for about 1 min). Following the above procedure, circular ($r \approx 25$ mm) and rectangular (3cm × 1cm) specimens of t ≈ 0.5 mm thickness were formed. The final concentration of the MWCNT in the samples varied from 0 to 8.0 wt.%.

2. 2. Experimental techniques

The morphological analysis was done by scanning electron microscopy (SEM) (Field Emission Electron Microscope Zeiss Gemini ULTRA plus, Carl Zeiss NTS GmbH). The pressed plates were cryo-fractured or cut and smoothed by an ultramicrotome. The smoothed surfaces were etched with THF for different times to improve the visibility of the MWCNT. All SEM samples were sputtered with platinum to hinder charging during the analysis.

Differential scanning calorimetry (DSC) measurements were carried out in the temperature range 30 to 230°C in nitrogen atmosphere, using a Perkin–Elmer Pyris 6 apparatus. Both cooling and heating rates were 10 K/min. The weight of the samples varied from 4 to 6 mg. It is noted that all the examined samples were formerly heated from room temperature to 230°C, at 10 K/min, and kept to that temperature for 5 min in order to remove any previous thermal history.

Dynamic-mechanical analysis (DMA) was performed by means of an Q800 (TA Instruments, USA) in the single cantilever mode with an oscillating amplitude of 10 μm at a frequency of 1 Hz in the temperature range from -50 to 150 °C (heating rate: 3 K/min.). 5 mm broad samples were cut from the 0.5 mm thick plates. The free sample length between the clamps was 10 mm.

Dielectric relaxation spectroscopy (DRS) measurements were carried out in the frequency range 10^{-2}–10^{6} Hz and the temperature range -150 to 170 ºC by means of a Novocontrol Alpha analyzer. The temperature was controlled to better than 0.1 K with a Novocontrol Quatro system. Golden electrodes were sputtered on both sides of the round

specimens to assure good electrical contact between these and the gold-plated capacitor plates. Further details about the method can be found in refs. [35,36].

Four-point probe *dc* conductivity measurements were conducted on the rectangular specimens using the combination of a Keithley 6220 high precision current source and a Keithley 2182A nanovoltmeter. The four probes were positioned along a straight line, with spacing s = 8 mm. A current (I) is passed through the sample via the outer probes (force probes) and the voltage (V) is measured at the inner probes (sense probes). The resistivity (ρ) is then obtained by the following equation [37]:

$$\rho = 2\pi \cdot F \cdot s \cdot R \tag{1}$$

where R is the resistance ($R=V/I$) and F a correction factor depending on the sample geometry (sample thickness, t, and distances from the edges of the sample) [38]. For $s >> t$, F can be expressed as:

$$F = \frac{t}{2(\ln 2)s} \tag{2}$$

Good electrical contacts between the sample surface and the probes were assured again by sputtering.

3. Results and discussion

3. 1. Morphological Characterization

Fig. 1 represents the morphologies of compression molded composites containing different amounts of MWCNT. Fractured surfaces of highly filled composites (5 wt.% MWCNT) show a homogeneous distribution of CNT on the surface (Fig. 1-a). Inhomogeneities are hardly detectable due to the rough fracture structure. Contrarily, when

the cuts were smoothed by means of a microtome (Fig. 1-b) the MWCNT appear just as bright dots, since they are cut at the same level like the matrix, and inhomogeneities in the density of the CNT packing become visible. The best image of the MWCNT distribution was obtained when the smoothed cut surface was etched with THF for some time, here shown for 0.5 to 5.0 wt.% (Figs. 1-c to 1-f). Due to the dissolution of the polymer surface the CNT appear as elevated structures clearly showing their widely homogeneous distribution in the PMMA matrix. With increasing amount of filler bigger spherical areas of agglomerated MWCNT are detectable in the dimension of > 10 µm (Figs. 1-c to 1-f). At lower MWCNT content also some agglomerates but with much smaller size and in lower concentration could be observed. Obviously, the mixing conditions are not sufficient to result in a perfect deagglomeration of the primary MWCNT agglomerates, but once the CNT are deagglomerated they distribute homogenously in the PMMA matrix. It is to mention that the analysis of the produced strands revealed very similar morphologies, indicating that the MWCNT distribution obtained by melt mixing remains unaffected during the compression molding step.

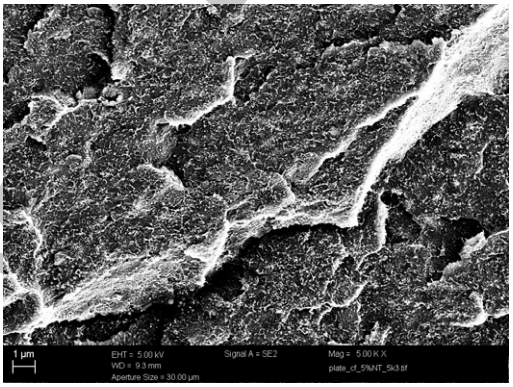

1-a
PMMA/5.0 wt.% MWCNT
cryo fracture

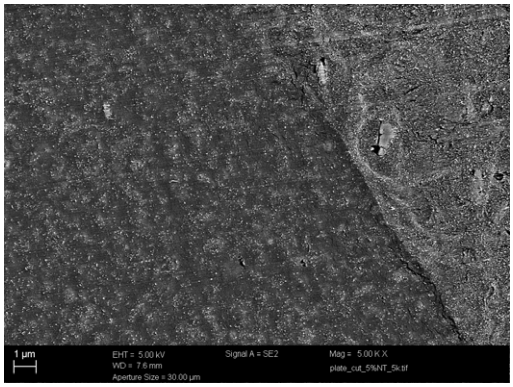

1-b
PMMA/5.0 wt.% MWCNT
smoothed cut

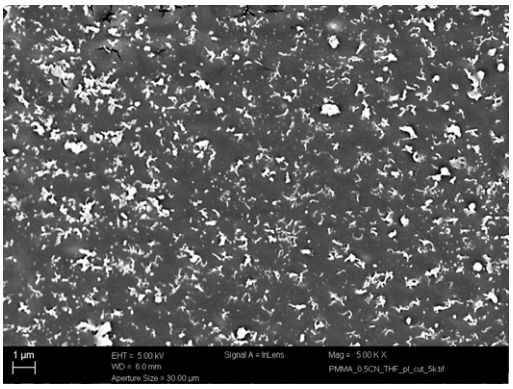

1-c
PMMA/0.5 wt.% MWCNT
smoothed cut, THF 30 s

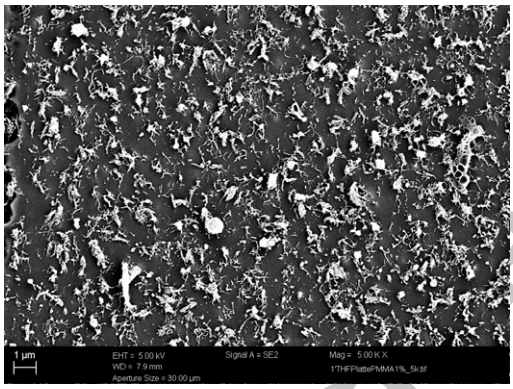

1-d
PMMA/1.0 wt.% MWCNT
smoothed cut, THF 1 Min.

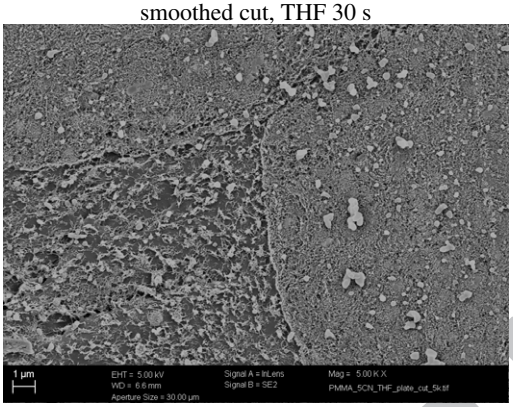

1-e
PMMA/5.0 wt.% MWCNT
smoothed cut, THF 30 s

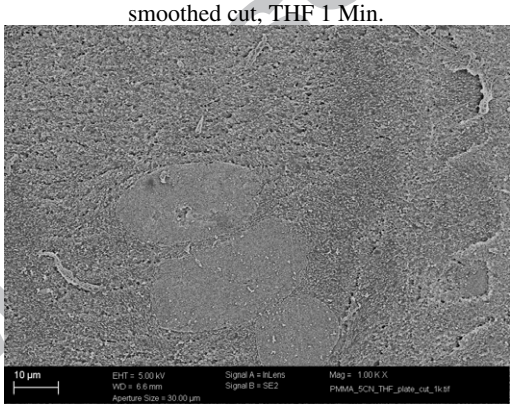

1-f
PMMA/5.0 wt.% MWCNT
smoothed cut, THF 30 s

Figure 1. SEM images of composites with different MWCNT concentrations (bar size = 1 μm). Images 1-a, 1-b and 1-e show the influence of the SEM sample preparation conditions on the appearance of the morphology. Figs. 1-c – 1-e show the influence of the MWCNT content on the homogeneity of their distribution. Fig. 1-f with lower magnification (bar size = 10 μm) reveals the size of the inhomogeneities.

3. 2. Thermal properties

The effects of MWCNT addition on the thermal properties of PMMA were examined by employing differential scanning calorimetry. DSC thermograms (second runs to erase any effects of thermal history) are shown in Fig. 2. The steps in heat flow, appeared at about 110 ºC, correspond to the glass transition of the amorphous matrix. A detailed analysis of the glass transition region is given in Table 1, where T_g is the glass transition temperature (calculated as the midpoint of the extrapolated heat capacities before and after

the glass transition), ΔC_p and ΔC_p^* are the heat capacity jump and the normalized to the polymer mass heat capacity jump ($\Delta C_p^* = \Delta C_p / (1-w)$, where w is the weight fraction of the MWCNT), respectively, and $\Delta T_g = T_{g,onset} - T_{g,end}$ the width of the glass transition ($T_{g,onset}$ and $T_{g,end}$ are defined as the intersections between the extrapolated tangents before and after the glass transition, respectively, and the extrapolated tangent at the inflection point). Generally, T_g of PMMA is strongly dependent on its stereoregularity. In particular, it ranges from 41.5 ºC, for high isotacticity ratios, to 125.6 ºC, as the atacticity increases [39]. Here the value of 107.9 ºC corresponds to PMMA where the syndiotactic tacticity dominates at a ratio of 0.56, with the rest 0.37 being atactic and 0.07 isotactic. As concerns the influence of MWCNT addition on the glass transition of PMMA the results of Table 1 show that no significant change is observed. Some deviations in T_g, ΔC_p^* and ΔT_g values are rather small and close to the experimental error and are not further discussed. The independence of both T_g and ΔC_p^* from the addition of CNT indicates weak polymer-filler interactions. This point will be further discussed in section 3.5, where the influence of the addition of MWCNT on the molecular dynamics of PMMA matrix is studied by DRS.

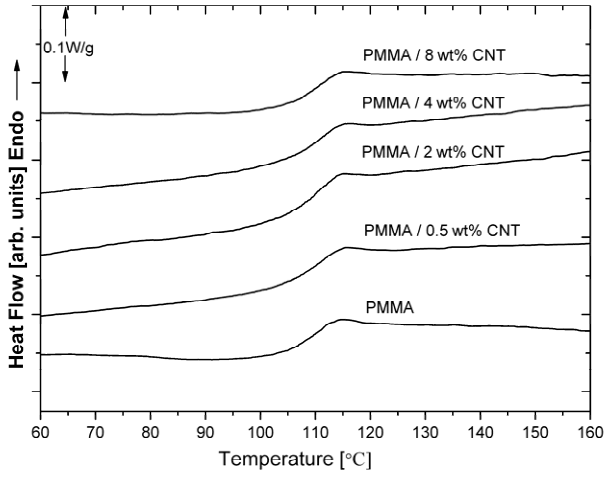

Figure 2. DSC thermograms (second runs) focused on the glass transition region for the samples indicated on the plot.

Table 1. Glass transition temperature (T_g), heat capacity jump (ΔC_p) and normalized heat capacity jump at T_g (ΔC_p^*), and glass transition width (ΔT_g) for the pure PMMA matrix and PMMA/MWCNT nanocomposites as obtained from DSC measurements. It is noted that the errors in temperatures are estimated to to ± 0.5 °C and in heat capacities to ± 0.05 J/g·ºC.

Sample	T_g (ºC)	ΔC_p (J/g·ºC)	ΔC_p^* (J/g·ºC)	ΔT_g (ºC)
PMMA	107.9	0.30	0.30	11.4
PMMA / 0.5 wt.% MWCNT	108.9	0.27	0.32	10.8
PMMA / 2.0 wt.% MWCNT	109.6	0.28	0.35	8.4
PMMA / 4.0 wt.% MWCNT	108.7	0.27	0.30	11.8
PMMA / 8.0 wt.% MWCNT	108.9	0.27	0.36	10.6

3. 3. Dynamic-mechanical properties

To analyze the influence of MWCNT on the mechanical behaviour of PMMA, DMA measurements have been performed. Table 2 contains the values of the storage and loss moduli at room temperature (25 °C) and the temperature of the tan δ peak maximum at the glass-rubber transition ($T_{g,DMA}$) of the composites in dependence on the MWCNT content. In all samples the glass transition occurs at around 121 °C, which is in the accuracy limit of ± 1 °C. It is noted that the T_g values determined by DMA are higher than these determined by DSC measurements. This is attributed to the higher frequency of measurements in DMA (1 Hz) against an equivalent frequency in DSC in the range 10^{-2} – 10^{-3} Hz [40]. Also, there is no tendency in the mechanical properties as function of the MWCNT content detectable. The scatter in the values of the moduli is in the range of the accuracy limit of ± 10 %. In agreement with the DSC results, and the later discussed DRS results, we can conclude that there are no strong matrix-filler interactions in the composites, which would result in increased moduli and mechanical strength. It is worth to be mentioned that in our previous works in other thermoplastics, but semicrystalline, matrices containing MWCNT and prepared following a similar procedure (isotactic polypropylene in ref. [41] and polyamide 6 in ref. [42]), a significant improvement in the storage modulus

was found by the addition of the nanotubes when a crystalline polymer layer (*trans*-crystallinity) had been developed around the MWCNT walls. The existence of this layer is beneficial concerning the mechanical properties, since it intervenes between the matrix and the embedded nanotubes, transferring the loads from the amorphous phase to the stiff fillers.

Table 2. Storage modulus (G'), loss modulus (G''), glass transition (determined as tan δ peak maximum, $T_{g,DMA}$), and tan δ at $T_{g,DMA}$ for pure PMMA and PMMA/MWCNT nanocomposites as obtained from DMA measurements.

Sample	G' @ 25°C (GPa)	G'' @ 25°C (MPa)	$T_{g,DMA}$ (°C)	tan δ at $T_{g,DMA}$
PMMA	3.72	270	121.5	0.80
PMMA / 0.5 wt.% MWCNT	3.36	219	121.0	1.24
PMMA / 1.0 wt.% MWCNT	3.99	250	121.1	0.86
PMMA / 3.0 wt.% MWCNT	3.86	244	122.3	0.83
PMMA / 5.0 wt.% MWCNT	3.25	209	121.4	0.49

3. 4. Electrical properties

The electrical properties of the prepared samples, and especially the electrical percolation threshold, were studied initially using dielectric relaxation spectroscopy (DRS). Fig. 3 shows the frequency (f) dependence of the real part of the complex electrical conductivity, $\sigma'(f)$, for the pure PMMA and the nanocomposites containing various MWCNT contents, measured at room temperature. Depending on the nanotubes concentration two distinct behaviours are observed. For the pure matrix, as well as for PMMA/0.5 wt.% MWCNT, *ac* conductivity increases linearly with the frequency, showing a typical behaviour for insulating materials. On the contrary, samples with loadings of at least 0.75 wt.% MWCNT exhibit a *dc* plateau, corresponding to *dc* conductivity (σ_{dc}), where σ' is independent of frequency below a critical frequency (f_c). This independence of frequency, which is characteristic for conductive materials, is extended in the whole frequency range as the amount of MWCNT further increases. Concluding, the *ac*

conductivity measurements clearly show that the transition from the insulating to the conducting phase, the so-called percolation threshold (p_c), is observed between 0.5 and 0.7 wt.% MWCNT, followed by a sharp increase in conductivity of about seven orders of magnitude. It is also interesting to note that conductivity shows saturation for concentrations higher than 1.0 wt.% MWCNT. Furthermore, for the same concentrations, conductivity deviates from the expected behaviour: increase in σ_{dc} on increasing the amount of the conducting filler. The latter, and especially the observed drop in σ' for $f > 3\times10^4$ Hz, are indicative that the measurements are out of the upper experimental limit of the apparatus. In general, usage of *ac* measurements, with the sample in sandwich configuration, is advisable for conductivity levels lower than 10^{-2} S/cm. For highly conducting samples, *dc* conductivity measurements in the four probes configuration are suggested. For that reason the samples with concentrations higher than 1.0 wt.% MWCNT were re-measured. Fig. 4 presents all the results of σ_{dc} against the carbon nanotubes volume content (vol.%), obtained either from *ac* or *dc* measurements as the dotted line denotes. The conversion from wt.% to vol.% was done as described in ref. [41]. As it is clearly seen the irregularity of the σ_{dc} values in the case of the highly conducting composites observed by DRS measurements was overcome when the *dc* conductivity was measured by the four probes technique.

For the exact calculation of p_c the well known scaling law from percolation theory [43] was applied to the experimental data of Fig.4:

$$\sigma_{dc} \sim (p\text{-}p_c)^{t} \tag{3}$$

where σ_{dc} is the *dc* conductivity, p is the volume fraction of the filler, and t is a critical exponent related with the dimensionality of the investigated system. The best fit was

achieved for p_c = 0.5 ± 0.1 vol.% (corresponding to 0.7 wt.%) and t = 1.8 ± 0.2 (solid line in Fig. 4). Even lower p_c values have been reported in PMMA/CNT systems prepared by other procedures like in-situ polymerization [8], solution casting [7,12,20-23] and others [27-29], without being able to make a direct comparison of these values since the aspect ratios of the nanotubes is not similar (in most of the cases they were in the range of 1000). For melt mixed polymer/CNT composites the obtained here electrical percolation threshold can be considered as low [5,44].

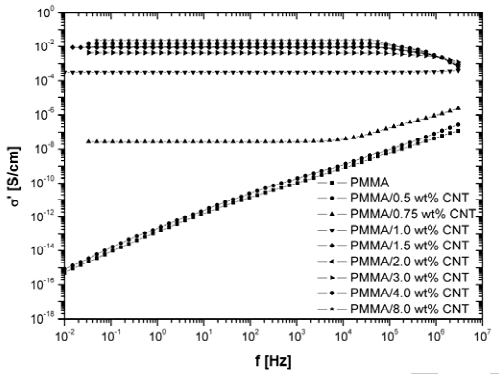

Figure 3. Conductivity (σ') vs frequency (f) at room temperature for the samples indicated on the plot.

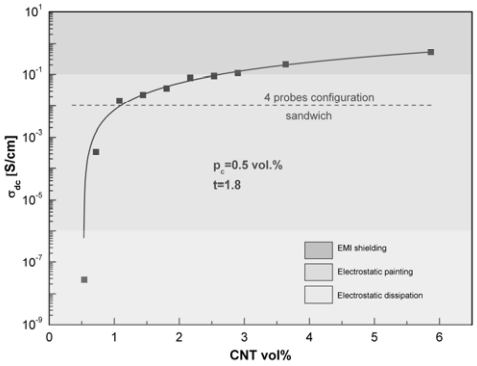

Figure 4. σ_{dc} vs MWCNT vol.% concentration for nanocomposites above p_c. The solid line corresponds to the best fit of Eq. 3 to the experimental values and the dotted line denotes the configuration of the dc conductivity measurements (sandwich or four probes).

As concerns the exponent t, the exported value of 1.8 is very close to the theoretically expected one for a statistical percolation network in three dimensions ($t \approx 2.0$), according to the percolation theory [45]. Indeed, recent studies based on Monte Carlo simulations in conducting systems containing randomly dispersed fillers with high aspect ratio showed that the conductivity exponent substantially decreases with the increase of the filler's aspect ratio [46]. Significant higher t values have been also observed in literature (2.9 in poly(ethylene terephthalate) / MWCNT [47], 4.5 in isotactic polypropylene /

MWCNT [41], 8.4 in polyamide 6 / MWCNT [35], and others listed in a recent review by Bauhofer et al. [44]), mainly in semicrystalline systems. Balberg at al. showed that a wide inter-particle distance distribution can lead to non-universal high t values [48]. It has been proved in various semicrystalline systems [41,42,49], that a crystalline layer is developed around CNT (*trans*-crystallinity), prohibiting the direct contact between them and giving rise to the above mentioned description. On the contrary, in the present work the absence of crystallinity is compatible with the convergence of t to its theoretical value.

Another interesting point that should be further discussed is the considerable high σ_{dc} values, making the materials good candidates to cover applications from electrostatic dissipation to EMI shielding (Fig. 4). Even from 4.0 wt.% MWCNT (or 2.9 vol.%) the criterion for EMI shielding is fulfilled ($\sigma_{dc} > 10^{-1}$ S/cm). The maximum value of conductivity ($\sigma_{dc,max}$ = 0.5 S/cm at 8.0 wt.% MWCNT) is one of the highest reported in literature so far (please compare with Bauhofer et al. where more than 150 systems are summarized, including their maximum conductivity values [44]). To further follow this point, the σ_{dc} values of several amorphous and semicrystalline systems, at various MWCNT contents, were collected from the literature [50-60] and summarized in Fig. 5. In order to eliminate any effects caused by the filler type, all the results included in Fig. 5 refer to systems prepared using the same type of MWCNT (Nanocyl^{TM} NC 7000). Even if nanocomposites preparation methods and conditions may differ, a general tendency can be observed at all the presented MWCNT contents: amorphous systems (open symbols) exhibit higher conductivity levels compared to the semicrystalline ones (solid symbols). The deviation of PMMA containing 1wt.% MWCNT is attributed to the fact that this concentration is very close to the p_c (0.7 wt.%) and consequently the percolated network is

still not well established. PCL appears to be an exception among the semicrystalline polymers, giving values in the range of the amorphous ones. PA6.6 and PP are also reaching the lowest levels of the amorphous systems. Fewer points corresponding to semicrystalline systems appear at the low concentrations since the systems are still below their electrical percolation threshold. The presented results manifest the importance of crystallinity in polymer/CNT nanocomposites. The absence of a crystalline layer, in particular around the CNT, allows a close approach of the conductive fillers rationalizing the high σ_{dc} values. It is interesting also to note that the maximum value obtained here is close to previously mentioned ones for MWCNT mats (~10-100 S/cm) [62,63].

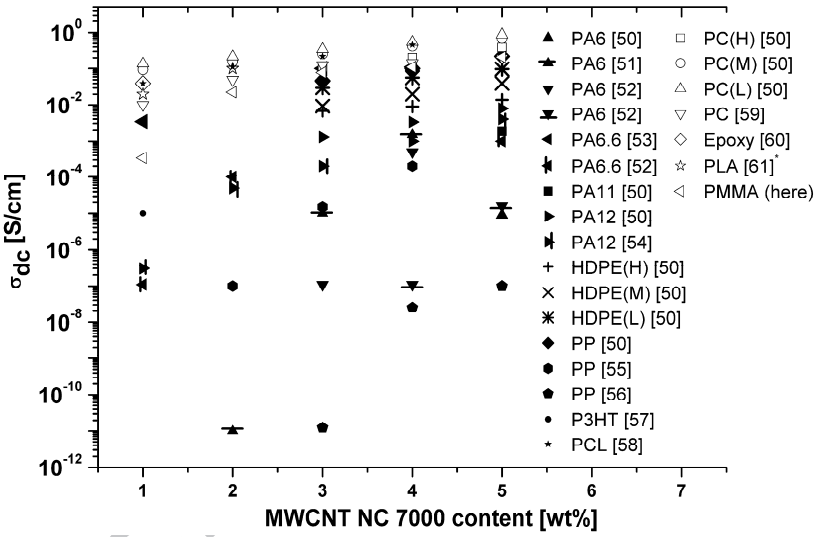

Acronyms: PA (polyamide), HDPE (high density polyethylene), PP (polypropylene), P3HT (poly 3-hexylthiophene), PCL (polycaprolactone), PC (polycarbonate), PMMA (polymethyl methacrylate), PLA (poly(lactic acid)). Letters H, M and L in parentheses correspond to high, medium and low molecular weight, respectively.

Figure 5. Conductivity values (σ_{dc}) at various MWCNT contents for several conducting polymer systems prepared using the same type of MWCNT (Nanocyl NC 7000). Open (right column in the legend) and solid symbols (left column in the legend) signify amorphous and semicrystalline systems, respectively.
* The usually semicrystalline PLA has been included to the amorphous polymers here, since its crystallinity was below 1.8% due to a fast cooling process during preparation (details in ref. [61]).

Weak polymer-filler interactions and absence of crystallinity assist the achievement of high conductivity levels. Work in progress on the conductivity mechanism by investigating the temperature dependence of conductivity, starting from low temperatures, in various

conductive polymer/CNT systems (amorphous or semicrystalline, having strong or weak polymer-filler interactions) clearly shows the importance of the mentioned above parameters with respect to the mechanism which controls the transport of the charge carriers (hopping or tunneling). These findings will be presented in the near future.

The theoretical p_c value can be also calculated using the excluded volume theory. In the case of inclusions with large aspect ratios, such as carbon nanotubes, the aspect ratio is correlated with the percolation threshold through the following equation [46]:

$$(l/d)\, p_c \approx 0.6 \quad (4)$$

By taking the dimensions of the MWCNT used in this study (l = 1.5 μm and d = 9.5 nm), the theoretically expected p_c is found to be ≈ 0.4 vol.%, a value which is very close to the experimentally exported one of 0.5 vol.%. This accordance suggests that both the preparation procedure (melt mixing) and conditions (230 ºC, 10 min, 100 rpm) were appropriate for the preparation of the nanocomposites. Nevertheless, it should be noted that the obtained theoretical p_c value can be only considered as a rough estimation and not as the absolute lower limit of the p_c, since the theory refers to well defined randomly distributed fillers (prisms, ellipsoids, cylinders, sticks) and also does not takes into account any polymer-filler and filler-filler interactions [64].

3. 5. Dielectric properties

The influence of the addition of MWCNT on the molecular mobility mechanisms of the PMMA matrix was studied by employing dielectric relaxation spectroscopy. The measurements were conducted isothermally at steps of 10 K, from -150 to 110 ºC, and at steps of 5 K, from 110 to 170 ºC. Figs. 6-a, 6-b and 6-c show the imaginary part (ε'') of

dielectric permittivity (dielectric loss) as a function of frequency (f) for pure PMMA. In particular, the observed peak at the low temperature range (Fig. 6-a) corresponds to the γ secondary dielectric relaxation mechanism of PMMA and is attributed to rotational motion of the CH_2 segments attached to either the main chain or to the ester side groups [65]. This particular relaxation appears to be weak due to the non polar nature of the methyl groups. As the temperature increases gradually from -150 to 0 ºC γ relaxation shifts to higher frequencies whereas at the same time, for T > -20 ºC, a second and stronger secondary relaxation, named β, appears at the low frequency side (Fig. 6-b), related to the hindered rotation of the ester side groups attached to the main chain [65]. Finally, from 110 to 125 ºC the main α relaxation mechanism, which is associated with the glass transition, comes into the frequency window and merges very fast with the particularly strong β relaxation at higher temperatures (Fig. 6-c) [66]. The high ε″ values at the low frequency side, with a slope of -1, arising from the onset of conductivity at temperatures round and above T_g [67].

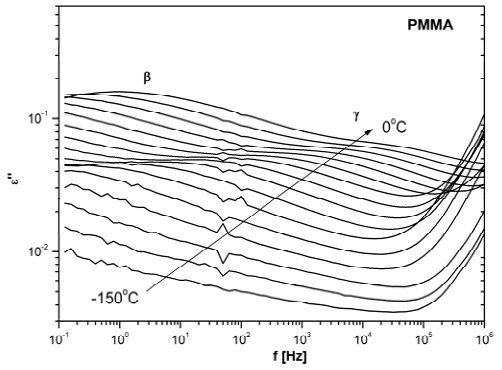

5-a

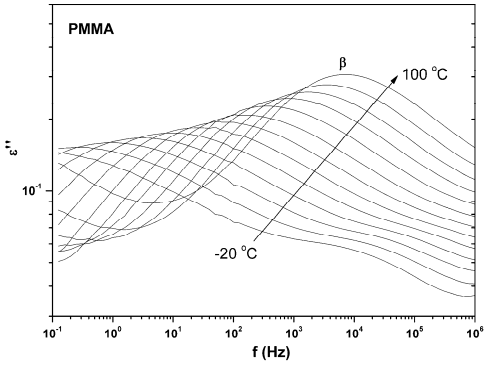

5-b

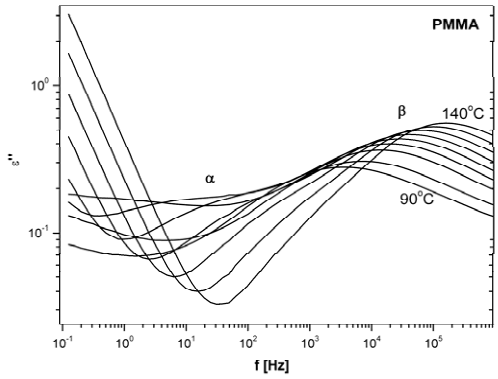

5-c

Figure 6. Imaginary part of the dielectric function (ε'') versus frequency (f) at the temperature range of γ (5-a), β (5-b) and α relaxation (5-c) for the pure PMMA.

Similar measurements were done for the nanocomposite containing 0.5 wt.% MWCNT. In order to study the influence of carbon nanotubes addition on the molecular dynamics of PMMA matrix in Fig. 7 selected temperatures of ε'' against f are presented for both the PMMA matrix and the PMMA/0.5 wt.% MWCNT nanocomposite. To further facilitate the investigation, in Fig. 8 comparative isochronal diagrams (ε'' against T at a fixed frequency of 20 Hz) for the mentioned above samples are shown. From the results, it is concluded that the addition of carbon nanotubes does not influence either the secondary (β and γ) or the main α relaxation mechanism of PMMA. Their position (typical relaxation times), shape and intensity remain practically unaffected. The only reported change is an overall slight increase of ε'' by the addition of MWCNT, which may be attributed to an enhancement of the internal field induced by the presence of the conducting fillers [68]. The same behavior has been reported previously for polyamide 6 matrix containing multi-walled carbon nanotubes [35]. The independence of the relaxations mechanisms of PMMA upon MWCNT addition is indicative of weak polymer-filler interactions and is consistent with the calorimetry and DMA findings. It is noted that the investigation was focused only on the sample containing 0.5 wt.% MWCNT, since it was the only non conductive

nanocomposite. An even more systematic study will be performed in the future preparing more samples below the percolation threshold.

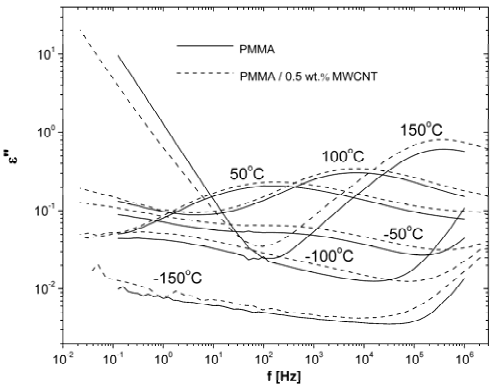

Figure 7. Imaginary part of the dielectric function (ε'') versus frequency (f) at the selected temperatures indicated on the plot, for pure PMMA and PMMA/0.5 wt.% MWCNT nanocomposite.

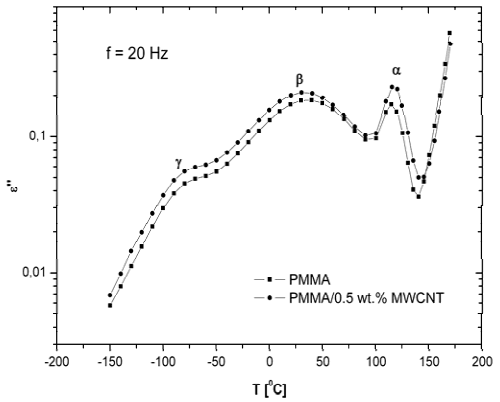

Figure 8. Imaginary part of the dielectric function (ε'') versus temperature (T) at a frequency of 20 Hz for pure PMMA and PMMA/0.5 wt.% MWCNT nanocomposite.

4. Conclusions

Multi-walled carbon nanotubes were incorporated by melt mixing in a poly(methyl methacrylate) matrix, with the aim to achieve high levels of bulk conductivity capable to fulfill a wide range of applications, from electrostatic dissipation to EMI shielding. Scanning electron microscopy results revealed a homogeneous dispersion and distribution of the nanoparticles into the polymer matrix with only a small extent of remaining primary agglomerates. The electrical properties of the nanocomposites containing various amounts of MWCNT were investigated by employing AC and DC conductivity measurements. The electrical percolation threshold (p_c) was determined to 0.5 vol.% MWCNT with a critical exponent t = 1.8 from DC conductivity values (σ_{dc}) using the scaling law of percolation theory. In addition, considerably high conductivity levels were achieved at relatively low MWCNT amounts: σ_{dc} exceeds 10^{-2} S/cm already at 1.1 vol.%, the criterion for EMI shielding ($\sigma_{dc} > 10^{-1}$ S/cm) is fulfilled at 2.9 vol.%, and σ_{dc} is 0.5 S/cm at the highest loaded sample (5.2 vol.%).

To further explore the structure – property relationships of the prepared nanocomposites their thermal, mechanical and dielectric properties were studied by

employing differential scanning calorimetry, dynamic mechanical analysis and dielectric relaxation spectroscopy, respectively. The independence of: (i) the glass transition temperature (T_g) and the normalized to the polymer mass heat capacity jump (ΔC_p^*), (ii) the storage modulus and the position of the tan δ peak, and mainly (iii) the dielectric relaxation mechanisms of the PMMA matrix by the addition of CNT, are all indicative of weak polymer – filler interactions in the nanocomposites. As it was extensively discussed, weak polymer – filler interactions and absence of crystallinity are both very crucial parameters which assist the achievement of high conductivity levels, since a closer approach of the conductive fillers in the developed network is allowed.

Acknowledgements

The research leading to these results has received partial support from the European Community's Seventh Framework Programme [FP7/2007-2013] under grant agreement no 218331 NaPolyNet (www.napolynet.eu). The authors acknowledge Professor E. Syskakis, University of Athens, who provided the necessary equipment for sputtering, and Dr. R. Häßler and Mr. H. Kunath (IPF Dresden) for DMA analysis and general technical assistance, respectively.

References

1. Marx W, Barth A. Carbon nanotubes – A scientometric study. Phys Status Solidi B 2008;245(10):2347-51.
2. Moniruzzaman M, Winey KI. Polymer nanocomposites containing carbon nanotubes. Macromolecules 2006;39(16):5194-5205.
3. Breuer O, Sundararaj U. Big returns from small fibers: A review of polymer/carbon nanotube composites. Polym Compos 2004;25(6):630-45.
4. Ajayan PM, Stephan O, Colliex C, Trauth D. Aligned carbon nanotube arrays formed by cutting a polymer resin-nanotube composite. Science 1994;265:1212-4.
5. Spitalsky Z, Tasis D, Papagelis K, Galiotis C. Carbon nanotube-polymer composites: Chemistry, processing, mechanical and electrical properties. Prog Polym Sci 2010;35(3):357-401.
6. Coleman JN, Khan U, Blau WJ, Gun'ko YK. Small but strong: A review of the mechanical properties of carbon nanotube-polymer composites. Carbon 2006;44(9):1624-52.
7. Kim HM, Kim K, Lee CY, Joo J, Cho SJ, Yoon HS, Pejakovic DA, Yoo JW, Epstein AJ. Electrical conductivity and electromagnetic interference shielding of multiwalled carbon nanotube composites containing Fe catalyst. Appl Phys Lett 2004;84(4):589-91.
8. Yuen SM, Ma CCM, Chuang CY, Yu KC, Wu SY, Yang CC, Wei MH. Effect of processing method on the shielding effectiveness of electromagnetic interference of MWCNT/PMMA composites. Compos Sci Technol 2008;68(3-4):963-8.
9. Huang YL, Yuen SM, Ma CCM, Chuang CY, Yu KC, Teng CC, Tien HW, Chiu YC, Wu SY, Liao SH, Weng FB. Morphological, electrical, electromagnetic interference

(EMI) shielding, and tribological properties of functionalized multi-walled carbon nanotube/poly methyl methacrylate (PMMA) composites. Compos Sci Technol 2009;69(11-12):1991-6.
10. Schmidt RH, Kinloch IA, Burgess AN, Windle AH. The Effect of Aggregation on the Electrical Conductivity of Spin-Coated Polymer/Carbon Nanotube Composite Films. Langmuir 2007;23:5707–12.
11. Kim DO, Lee MH, Lee JH, Lee TW, Kim KJ, Lee YK, Kim T, Choi HR, Koo JC, Nam JD. Transparent flexible conductor of poly(methyl methacrylate) containing highly-dispersed multiwalled carbon nanotube. Org Electron 2008;9(1):1-13.
12. Dettlaff-Weglikowska U, Kaempgen M, Hornbostel B, Skakalova V, Wang JP, Liang JD, Roth S. Conducting and transparent SWCNT/polymer composites. Phys Stat Sol B 2006;243(13):2440-4.
13. Li Y, Wang XC, Yang MJ. n-Type gas sensing characteristics of chemically modified multi-walled carbon nanotubes and PMMA composite. Sens Actuators, B 2007;121(2):496-500.
14. Shang S, Li L, Yang X, Wei Y. Polymethylmethacrylate-carbon nanotubes composites prepared by microemulsion polymerization for gas sensor. Compos Sci Technol 2009;69(7-8):1156-9.
15. Velasco-Santos C, Martínez-Hernández AL, Fisher FT, Ruoff R, Castaño VM. Improvement of Thermal and Mechanical Properties of Carbon Nanotube Composites through Chemical Functionalization. Chem Mater 2003;15:4470-5.
16. Ramanathan T, Liu H, Brinson LC. Functionalized SWCNT/polymer nanocomposites for dramatic property improvement. J Polym Sci Part B 2005;43(17):2269-79.
17. Wei HF, Hsiue GH, Liu CY. Surface modification of multi-walled carbon nanotubes by a sol–gel reaction to increase their compatibility with PMMA resin. Compos Sci Technol 2007;67(6):1018-26.
18. Wang M, Pramoda KP, Goh SH. Enhancement of interfacial adhesion and dynamic mechanical properties of poly(methyl methacrylate)/multiwalled carbon nanotube composites with amine-terminated poly(ethylene oxide). Carbon 2006;44(4):613-7.
19. McClory C, McNally T, Baxendale M, Pötschke P, Blau W, Ruether M. Electrical and rheological percolation of PMMA/MWCNT nanocomposites as a function of CNT geometry and functionality. Eur Polym J 2010;46(5):854-68.
20. Benoit JM, Corraze B, Lefrant S, Blau WJ, Bernier P, Chauvet O. Transport properties of PMMA-carbon nanotubes composites. Synth Met 2001;121(1-3):1215-6.
21. Chauvet O, Benoit JM, Corraze B. Electrical, magneto-transport and localization of charge carriers in nanocomposites based on carbon nanotubes. Carbon 2004;42(5-6):949-52.
22. Skakalova V, Dettlaff-Weglikowska U, Roth S. Electrical and mechanical properties of nanocomposites of single wall carbon nanotubes with PMMA. Synth Met 2005;152(1-3):349-52.
23. Chen H, Muthuraman H, Stokes P, Zou J, Liu X, Wang J, Huo Q, Khondaker SI, Zhai L. Dispersion of carbon nanotubes and polymer nanocomposite fabrication using trifluoroacetic acid as a co-solvent. Nanotechnology 2007;18(41):415606.
24. Dai J, Wang Q, Li W, Wei Z, Xu G. Properties of well aligned SWNT modified poly (methyl methacrylate) nanocomposites. Mater Lett 2007;61(1):27-29.

25. Park SJ, Kim ST, Cho MS, Kim HM, Joo J, Choi HJ. Electrical properties of multi-walled carbon nanotube/poly(methyl methacrylate) nanocomposite. Curr Appl Phys 2005;5(4):302-4.
26. Du F, Fischer JE, Winey KI. Coagulation method for preparing singlewalled carbon nanotube/poly(methyl methacrylate) composites and their modulus, electrical conductivity, and thermal stability. J Polym Sci B: Polym Phys 2003;41(24):3333-8.
27. Du F, Scogna RC, Zhou W, Brand S, Fischer JE, Winey KI. Nanotube networks in polymer nanocomposites: rheology and electrical conductivity. Macromolecules 2004;37:9048-55.
28. Sundaray B, Subramanian V, Natarajan TS, Krishnamurthy K. Electrical conductivity of a single electrospun fiber of poly(methyl methacrylate) and multiwalled carbon nanotube nanocomposite. Appl Phys Lett 2006;88:143114.
29. Regev O, ElKati PNB, Loos J, Koning CE. Preparation of Conductive Nanotube-Polymer Composites Using Latex Technology. Adv Mater 2004;16(3):248-51.
30. Haggenmueller R, Gommans HH, Rinzler AG, Fischer JE, Winey KI. Aligned single-wall carbon nanotubes in composites by melt processing methods. Chem Phys Lett 2000;330(3-4):219-25.
31. Jin Z, Pramoda KP, Xu G, Goh SH. Dynamic mechanical behavior of melt-processed multi-walled carbon nanotubes/poly(methyl methacrylate) composites. Chem Phys Lett 2001;337(1-3):33-47.
32. Gorga RE, Cohen RE. Toughness enhancements in poly(methyl methacrylate) by addition of oriented multiwall carbon nanotubes. J Polym Sci B: Polym Phys 2004;42(14):2690-2702.
33. Inam F, Yan H, Reece MJ, Peijs T. Dimethylformamide: an effective dispersant for making ceramic-carbon nanotube composites. Nanotechnology 2008;19:195710.
34. Material data sheet NC7000, Nanocyl S.A. Sambreville, Belgium, 05 February 2007.
35. Logakis E, Pandis Ch, Peoglos V, Pissis P, Pionteck J, Pötschke P, Mičušik M, Omastová M. Electrical/dielectric properties and conduction mechanism in melt processed polyamide/multi-walled carbon nanotubes composites. Polymer 2009;50(21):5103-11.
36. Kremer F, Schoenhals A. Broadband Dielectric Spectroscopy, Germany: Springer, 2002.
37. Schroder DK. Semiconductor material and device characterization. New Jersey: Wiley, 3rd ed., 2006.
38. Smits FM. Measurement of sheet resistivities with 4-point probe. The Bell System Technical Journal 1958;37(3):711-718.
39. Brandrup J, Immergut EH, Grulke EA, Abe A, Bloch DR. Polymer Handbook. John Wiley & Sons, 1999.
40. Vatalis AS, Kanapitsas A, Delides CG, Pissis P. Relaxation phenomena and morphology in polymer blends based on polyurethanes investigated by various techniques. Thermochim Acta 2001;372(1-2):33-38.
41. Logakis E, Pollatos E, Pandis Ch, Peoglos V, Zuburtikudis I, Delides CG, Vatalis A, Gjoka M, Syskakis E, Viras K, Pissis P. J. Structure-property relationships in isotactic polypropylene/multi-walled carbon nanotubes nanocomposites. Comp Sci Technol 2010;70(2):328-35.

42. Logakis E, Pandis Ch, Peoglos V, Pissis P, Stergiou Ch, Pionteck J, Pötschke P, Mičušik M, Omastová M. Structure–Property Relationships in Polyamide6/Multi-Walled Carbon Nanotubes Nanocomposites. J Polym Sci Part B 2009;47(8):764-74.
43. Stauffer D, Aharony A. Introduction to percolation theory. Taylor & Francis, 2nd Revised Edition, 2003.
44. Bauhofer W, Kovacs JZ. A review and analysis of electrical percolation in carbon nanotube polymer composites. Compos Sci Technol 2009;69(10):1486-98.
45. Gingold BD, Lobb CJ. Percolative conduction in three dimensions. Phys Rev B 1990;42:8220.
46. Foygel M, Morris RD, Anez D, French S, Sobolev VL. Theoretical and computational studies of carbon nanotube composites and suspensions: Electrical and thermal conductivity. Phys Rev B 2005;71:104201.
47. Logakis E, Pissis P, Pospiech D, Korwitz A, Krause B, Reuter U, Pötschke P. Low electrical percolation threshold in poly(ethylene terephthalate) / multi-walled carbon nanotube nanocomposites. Eur Polym J 2010;46(5):928-36.
48. Balberg I. A comprehensive picture of the electrical phenomena in carbon black–polymer composites. Carbon 2002;40(2):139-43.
49. Lu K, Grossiord N, Koning CE, Miltner HE, Van Mele B, Loos J. Carbon Nanotube/Isotactic Polypropylene Composites Prepared by Latex Technology: Morphology Analysis of CNT-Induced Nucleation. Macromolecules 2008;41:8081.
50. Ha H, Ha KR, Kim SC. An empirical equation for electrical resistivity of thermoplastic polymer/multi-walled carbon nanotube composites. Carbon 2010;48(7):1939-44.
51. Kodgire PV, Bhattacharyya AR, Bose S, Gupta N, Kulkarni AR, Misra A. Control of multiwall carbon nanotubes dispersion in polyamide6 matrix: an assessment through electrical conductivity. Chem Phys Lett 2006;432(4-6):480–5.
52. Krause B, Pötschke P, Häußler L. Influence of small scale mixing conditions on electrical resistivity of carbon nanotube-polyamide somposites. Compos Sci Technol 2009;69(10):1505-15.
53. Krause B, Petzold G, Pegel S, Pötschke P. Correlation of carbon nanotube dispersability in aqueous surfactant solutions and polymers. Carbon 2009;47(3):602-12.
54. Socher R, Krause B, Boldt R, Hermasch S, Wursche R, Pötschke P. Melt mixed nanocomposites of PA12 with MWCNTs: Influence of MWCNT and matrix properties on macrodispersion and electrical properties. Compos Sci Technol 2011;71(3):306-14.
55. M. Mičušík, M. Omastová, J. Pionteck, Ch. Pandis, E. Logakis, P. Pissis. Influence of surface treatment of multiwall carbon nanotubes on the properties of polypropylene/carbon nanotubes nanocomposites. Polym Adv Technol 2011;22:38-47.
56. Pötschke P, Krause B, Stange J, Münstedt H. Elongational viscosity and foaming behavior of PP modified by electron irradiation or nanotube addition. Macromol Symp 2007;254(1):400-8.
57. Musumeci AW, Silva GG, Liu JW, Martens WN, Waclawik ER. Structure and conductivity of multi-walled carbon nanotube/poly(3-hexylthiophene) composite films. Polymer 2007;48(6):1667-78.
58. Villmow T, Kretzschmar B, Pötschke P. Influence of screw configuration, residence time, and specific mechanical energy in twin-screw extrusion of

polycaprolactone/multi-walled carbon nanotube composites. Compos Sci Technol 2010;70(14):2045–55.
59. Pegel S, Pötschke P, Petzold G, Alig I, Dudkin SM, Lellinger D. Dispersion, agglomeration, and network formation of multiwalled carbon nanotubes in polycarbonate melts. Polymer 2008;49(4):974-84.
60. Kovacs JZ, Velagala BS, Schulte K, Bauhofer W. Two percolation thresholds in carbon nanotube epoxy composites. Compos Sci Technol 2007;67(5):922-8.
61. Villmow T, Pötschke P, Pegel S, Häussler L, Kretzschmar B. Influence of twin-screw extrusion conditions on the dispersion of multi-walled carbon nanotubes in a poly(lactic acid) matrix. Polymer 2008;49(16):3500–9.
62. Yang DJ, Wang SG, Zhang Q, Sellin PJ, Chen G. Thermal and electrical transport in multi-walled carbon nanotubes. Phys Lett A 2004;329(3):207-13.
63. Aliev AE, Guthy C, Zhang M, Fang S, Zakhidov AA, Fischer JE, Baughman RH. Thermal transport in MWCNT sheets and yarns. Carbon 2007;45(15):2880-8.
64. Saar MO, Manga M. Continuum percolation for randomly oriented soft-core prisms. Phys Rev E 2002;65:056131.
65. Clayton LM, Sikder AK, Kumar A, Cinke M, Meyyappan M, Gerasimov TG, Harmon JP. Transparent Poly(methyl methacrylate)/Single-Walled Carbon Nanotube (PMMA/SWCNT) Composites Films with Increased Dielectric Constants. Adv Funct Mater 2005;15(1):101-6.
66. Garwe F, Schönhals A, Lockwenz H, Beiner M, Schröter K, Donth E. Influence of Cooperative α Dynamics on Local β Relaxation during the Development of the Dynamic Glass Transition in Poly(n-alkyl methacrylate)s. Macromolecules 1996;29:247.
67. Neagu RM, Neagu E, Bonanos N, Pissis P. Electrical conductivity studies in nylon 11. J Appl Phys 2000;88(11):6669.
68. Kotsilkova R, Fragiadakis D, Pissis P. Reinforcement effect of carbon nanofillers in an epoxy resin system: Rheology, molecular dynamics, and mechanical studies. J Polym Sci Part B 2005;43(5):522-33.

Figure Captions

Figure 1. SEM images of composites with different MWCNT concentrations (bar size = 1 μm). Images 1-a, 1-b and 1-e show the influence of the SEM sample preparation conditions on the appearance of the morphology. Figs. 1-c – 1-e show the influence of the MWCNT content on the homogeneity of their distribution. Fig. 1-f with lower magnification (bar size = 10 μm) reveals the size of the inhomogeneities.

Figure 2. DSC thermograms (second runs) focused on the glass transition region for the samples indicated on the plot.

Figure 3. Conductivity (σ') vs frequency (f) at room temperature for the samples indicated on the plot.

Figure 4. σ_{dc} vs MWCNT vol.% concentration for nanocomposites above p_c. The solid line corresponds to the best fit of Eq. 3 to the experimental values and the dotted line denotes the configuration of the dc conductivity measurements (sandwich or four probes).

Figure 5. Conductivity values (σ_{dc}) at various MWCNT contents for several conducting polymer systems prepared using the same type of MWCNT (Nanocyl NC 7000). Open (right column in the legend) and solid symbols (left column in the legend) signify amorphous and semicrystalline systems, respectively.

Figure 6. Imaginary part of the dielectric function (ε'') versus frequency (f) at the temperature range of γ (5-a), β (5-b) and α relaxation (5-c) for the pure PMMA.

Figure 7. Imaginary part of the dielectric function (ε'') versus frequency (f) at the selected temperatures indicated on the plot, for pure PMMA and PMMA/0.5 wt.% MWCNT nanocomposite.

Figure 8. Imaginary part of the dielectric function (ε'') versus temperature (T) at a frequency of 20 Hz for pure PMMA and PMMA/0.5 wt.% MWCNT nanocomposite.